RSC Applied Polymers

ROYAL SOCIETY OF CHEMISTRY

PAPER

View Article Online
View Journal | View Issue

Cite this: *RSC Appl. Polym.*, 2025, **3**, 845

Bespoke polyamides *via* post-polymerization modification using accessible bioadvantaged monounsaturated long chain fatty acid units†

Peter M. Meyer,[a] Dhananjay Dileep,[a] Risha L. Bond,[b] Fasil A. Tadesse,[b] Michael J. Forrester [a] and Eric W. Cochran *[a]

Here, we report the copolymerization of a C20:1 monounsaturated long-chain α,ω (MULCH) diacid with polyamide-6,6 (PA66) and polyamide-6 (PA6), and subsequent post-polymerization derivatizations in the swollen or solid state. Surprisingly, most of the unsaturation survived harsh polymerization conditions. The partially unsaturated polyamides were subsequently derivatized through swollen- or solid-state chemistries, including epoxidation and thiol–ene click reactions, demonstrating the opportunity to transform a single nylon/MULCH copolymer into a plethora of high-performance specialty grades through processes like reactive extrusion or chemical washing. Bio-based MULCH diacids could thus serve as a foundation for bespoke polyamides; for example, enabling enhanced water resistance, crosslinkability, recyclability, or internal plasticization. The versatility afforded by MULCH diacid monomers adds significant value, supporting the growth of the bioeconomy. We illustrate these concepts with several examples of modifying MULCH copolymers: chemical staining, enhanced hydrophobicity through grafting of aliphatic pendants, crosslinking, and epoxidation. Chemical and physical properties are evaluated and compared to those of PA66 or PA6 homopolymer controls. Advances in vegetable oil processing and biotechnology have enabled the large-scale production of a variety of MULCH-diacids from lignocellulosic feedstocks. This work illustrates how the "bioadvantage" presented by monounsaturation can be exploited in high-value applications, facilitating the growth of the biobased chemical sector.

Received 4th February 2025,
Accepted 24th March 2025

DOI: 10.1039/d5lp00030k

rsc.li/rscapplpolym

1 Introduction

Polyamides, a key class of semi-crystalline engineering thermoplastics, have been foundational to materials engineering since their inception in the 1930s.[1,2] Polyamides demonstrate excellent thermomechanical properties and chemical resistance, owing to the hydrogen bond between neighboring backbone amide linkages. This unique feature has propelled polyamides into a wide array of applications, ranging from automotive and textile industries to electrical components and machinery parts,[3] and even extending into specialized sectors like biomedical devices.[4,5] To fine-tune their properties, industry typically varies the interamide carbon chain length to tune the thermomechanical characteristics and amide linkage density.[6,7] While specialized examples like DuPont's Kevlar™,[2,8] a polyaramid targeting highly specialized applications, are significant, the vast majority of commercial polyamides continue to be dominated by PA66 and PA6. This is largely due to superior mechanical performance and a robust infrastructure supporting these more conventional polyamides, ensuring their continued prevalence across various industries.

Polyamides can be readily differentiated through the incorporation of novel monomers to yield specialized materials tailored to address specific property requirements. Such novel materials often tackle inherent limitations of traditional polyamides, such as hydrophobicity and mechanical strength. Monomer differentiation through the addition and variation of pendant groups on aromatic[9–12] or aliphatic[13–15] repeat units has emerged as an efficient strategy for polyamide differentiation. For example, the processability of aromatic polyamides can be improved through the incorporation of bulky pendant groups,[12] or electro-switchable optical properties can be introduced through α/β-substituted naphthalene pendants.[13] In spite of the utility promised by these advanced

[a]*Department of Chemical & Biological Engineering, Iowa State University, Ames, Iowa 50011, USA. E-mail: ecochran@iastate.edu*
[b]*Geno, 4757 Nexus Center Drive, San Diego, CA, USA*

†Electronic supplementary information (ESI) available: Tabulated data, research photos, NMR spectra, and additional graphs. See DOI: https://doi.org/10.1039/d5lp00030k

materials, the resource intensity of designing them on a case-by-case basis poses significant barriers to widespread proliferation of bespoke polyamides. This limitation is echoed widely throughout the field; a recent review by Winnacker *et al.* highlights functionalization strategies aimed at increasing biocompatibility for medical uses, underscoring the narrow application range.[14] Thus, while novel monomers differentiated through their pendant-group chemistry offer a means to design polyamides with specific functionalities, the dependency on monomer customization rather than post-polymerization adjustments constrains the method's versatility.

Aside from polyamide differentiation, many research and commercial efforts are presently dedicated to improving polyamide sustainability through the development of bio-based feedstocks.[3,6,16–18] Recent advances in biotechnology have enabled engineered yeast and fungi to produce direct replacements for polyamide precursors from biomass.[19–27] Amongst the success stories is the commercial production of bio-caprolactam, bio-adipic acid, and bio-hexamethylenediamine (HMDA),[28,29] with lactams readily produced *via* fermentation in large quantities.[30] Research into partial bio-replacement has largely focused on bio-based diacids, leveraging their natural abundance.[31,32] While drop-in replacements require no technical adaptations, the fiercely competitive pricing offered by the petrochemical industry makes adoption a challenge, particularly as new biomanufacturing enterprises must recover capital investments and continue to seek process intensification.

Most biosynthetic metabolites require further chemical processing to yield the targeted drop-in replacement, increasing cost. Bio-adipic acid, for example, is one of many possible derivatives of *cis–cis*-muconic acid.[31,33] "Bio-advantaged" molecules, value-added molecules not practically obtainable through petrochemical means, may be identified by reducing the number of chemical processing steps.[34] This approach can reduce costs, while simultaneously affording novel biomonomers at the intersection of thrusts to improve both polyamide utility and sustainability. In the case of *cis–cis*-muconic acid, for example, partial hydrogenation through electrocatalysis yields 3-hexenedioic acid (HDA), a mono-unsaturated short chain (MUSH) diacid.[35,36] HDA is analogous to adipic acid, aside from the double bond that in principle offers a "bio-advantage" through a range of alkene chemistries available for subsequent derivatization including metathesis, thiol–ene addition, Michael addition, epoxidation, esterification, and others. If incorporated into the primary chain of polyamides, this unsaturation would offer a plethora of opportunities for *post-polymerization* specialization. Abdolmohammadi *et al.* demonstrated, however, the harsh conditions of polyamidation afforded *hydrated* HDA. Hadel *et al.* attempted several thiol–ene-based pendant group additions to HDA at the monomer stage; these efforts were frustrated by sluggish kinetics and the loss of thiol adducts during polymerization.[37] It was speculated the proximity of the double bond to the acyl groups created a unique electronic environment poorly suited to the desired chemistries. Based on this research, we speculated the monounsaturated *long*-chain (MULCH) fatty acids may be interesting comonomers for polyamides with their more aliphatic chemical environment and their emergence as viable biorefinery products. For instance, selective oxidation readily converts vegetable-oil based fatty acids into the corresponding MULCH diacids at industrial scales. While a complete LCA or TEA is beyond the scope of this study, we propose the work done on shorter MUSH[38–41] molecules such as *cis–cis*-muconic acid offers a reasonable estimate of industrial scalability. It has been demonstrated these bio-based molecules can be produced economically. The increase in price is offset by the ability of MULCH diacids to increase bio-content while simultaneously introducing valuable functionality, as demonstrated in Fig. 1.[42]

In this work, we hypothesized the aliphatic environment of the alkene in MULCH diacids would be less prone to hydration compared to HDA. We synthesized a model MULCH diacid through the metathesis of 10-undecenoic acid (C20:1) and prepared several C20:1 copolymers with both PA66 and PA6. We found most of the unsaturation survived the harsh conditions of polyamidation, enabling a range of post-polymerization modifications without necessitating the synthesis of new monomers. The capability for post-polymerization differentiation is a powerful tool directly addressing various challenges within the polyamide industry.

2 Results and discussion

2.1 Monomer synthesis and polymerization

The synthesis of a model C20:1 mono-unsaturated long chain polymer for partially unsaturated polyamides commenced with the Grubbs-mediated metathesis[43] of 10-undecenoic acid, chosen for its terminal alkene, to produce a long-chain diacid monomer with a central alkene. This monomer was then reacted with HMDA to form the 6,20:1 salt. The method facilitated a 65% conversion rate at a scale of 680 g. The purification involved sequential washes with cold and then hot hexane, yielding a final product with 99% purity, critical for ensuring the desired molecular weight of the polymer. This purified powder was subsequently converted into a polyamide "MULCH" salt, with ethyl alcohol as the solvent. The outcome of this process was a fluffy light yellow powder.

The MULCH salts were then mixed at various ratios with either adipic acid:HMDA salts or caprolactam and then melt polymerized to yield PA66 and PA6 copolyamides detailed in Table 1. For a fixed polymerization protocol, the GPC of PA66-MULCH-5, PA66-MULCH-10, and PA66-MULCH-40 shows decreasing molecular weight with increasing MULCH content. This inverse relationship, influenced by the high conversion third-order reaction kinetics,[44] means longer polymerization times are necessary due to decreased end group concentration. Specifically, PA66-MULCH-40 required solid-state polymerization to achieve the desired molecular weight, indicating insufficient residence time in the reactor. Further optimization was not attempted due to the complex nature of laboratory-

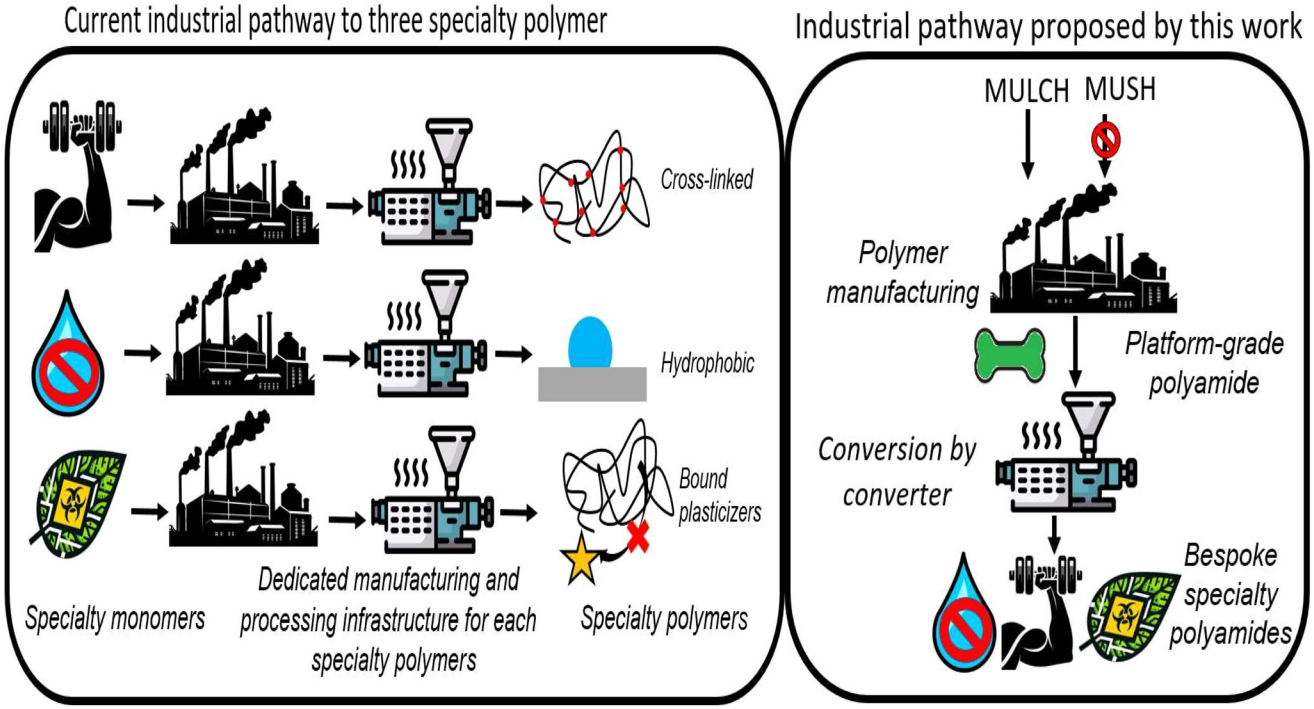

Fig. 1 Diagram demonstrating the two diverging pathways available to produce specialty polyamides: monomer differentiation and polymer differentiation.

Table 1 Molecular weight, mechanical properties, and water absorbance data for unmodified and modified polyamides

polyamide	M_n, kDa	M_w, kDa	D, none	UTS, MPa	Elongation, %	YM[a], GPa	Δwt[b], %
Neat dogbones[c]							
PA66	56.5	97.0	1.7	69.6 ± 4.9	132 ± 50	—	—
PA66-MULCH-5	45.5	111.0	2.4	96.7 ± 7.2	106 ± 38	—	—
PA66-MULCH-10	34.1	68.6	2.0	56.2 ± 6.0	150 ± 84	—	—
PA66-MULCH-40	11.2	28.0	2.5	—	—	—	—
Untreated fibers[d]							
PA66	51.9	96.2	1.9	71.35 ± 1.3	131 ± 1.2	2.4 ± 0.4	14.4
PA6	24.7	43.4	1.8	59.9 ± 4	95 ± 27	1.2 ± 0.6	11.5
PA66-Blend[e]	33.8	66.0	2.0	55.2 ± 0.7	132 ± 5	2.2 ± 0.6	8.6
PA6-MULCH-10	19.3	46.9	2.4	27.2 ± 0.1	66 ± 0.1	1.2 ± 0.1	7.0
Tetrakis treated fibers [d]							
PA66-SH_4	47.6	89.6	1.9	72.6 ± 7	160 ± 8	1.6 ± 0.2	10.1
PA6-SH_4	22.5	40.2	1.8	49.6 ± 0.7	120 ± 2.2	0.82 ± 0.5	12.1
PA66-Blend-SH_4	38.7	71.6	1.9	69.6 ± 0.05	144 ± 4.1	1.8 ± 0.5	10.1
PA6-MULCH-10-SH_4	20.5	61.3	3.0	35.9 ± 0.1	5.7 ± 0.1	1.4 ± 0.1	5.9
Dodecanethiol treated fibers[d]							
PA66-C12	49.7	92.7	1.9	73.5 ± 2.2	155 ± 10	1.1 ± 0.1	8.2
PA6-C12	23.4	40.9	1.8	53.4 ± 1.4	160 ± 17	0.83 ± 0.5	19.3
PA66-Blend-C12	37.2	68.6	1.8	71.6 ± 0.1	96 ± 0.1	2.0 ± 0.7	8.2
PA6-MULCH-10-C12	20.5	58.2	2.8	38.8 ± 0.1	39.1 ± 0.1	1.5 ± 0.1	5.6

[a] Young's modulus. [b] The change in weight due to water absorbance. [c] Conditioned at 55% RH for 24 hours. [d] Conditioned at 63% RH for 48 hours. [e] Blend created by creating a PA66-MULCH-40 copolymer and blending it with PA66 in a ratio of 5 to 1.

scale polyamidation and the limited quantity of the MULCH salt. A more detailed explanation, including optimization parameters, can be found in a previous paper published by the authors.[45] Despite reduced molecular weights, the copolymers maintained the polyamides' distinctive glossy finish, qualitatively suggestive of successful polymerization suitable for subsequent chemical and thermomechanical testing. ^{1}H NMR results demonstrated many of the alkene groups persisted through polymerization and melt processing (Fig. 2a), diverging from prior work done with HDA,[46] a MUSH, where hydrolysis eliminated the alkenes. The retention of alkenes was not absolute; after polymerization, PA66-MULCH-5 decreased to

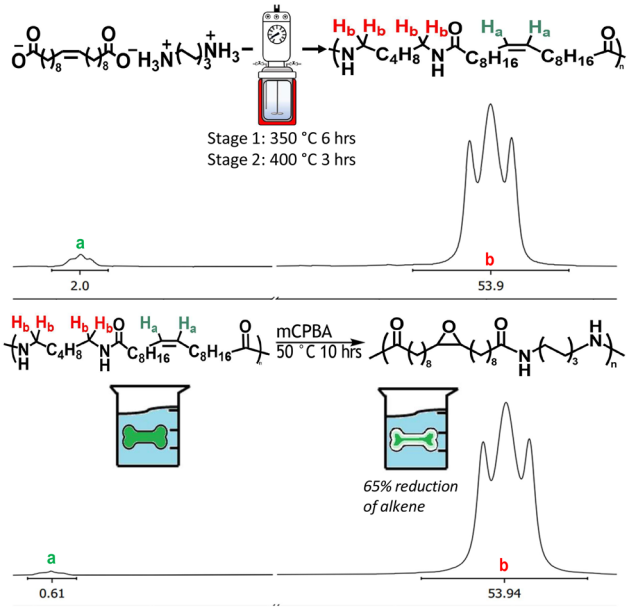

Fig. 2 (a) NMR of PA66-MULCH-10 showing retention of the alkene after polymerization and melt processing. Integration at 5.5 ppm corresponds to the product and is compared to the hydrogen alpha to the amine in HMDA at 3.8 ppm. (b) NMR of epoxidized polyamides. The integration at 5.5 ppm has decreased, demonstrating consumption of the alkene. Full spectra can be found in the ESI,† along with 5 mol% spectra.

4.1 mol% and further reduced to 3.0 mol% post-processing. Conversely, PA66-MULCH-10 dropped to 7.7 mol% after polymerization but maintained its alkene content during processing, suggesting appropriate processing methods can mitigate alkene loss. The resilience of alkenes in MULCH copolymers, unlike their behavior in HDA copolymers, reveals an electronic environment that resists hydrolysis. While long MULCH chains can undergo hydrolysis, the reaction appears to be suppressed. Two possible explanations are proposed: (1) the reverse reaction in MULCH occurs much more slowly than in MUSH or (2) the carbonyl group stabilizes a nearby water molecule, prolonging its presence and facilitating hydrolysis. Regardless of the exact mechanism, this phenomenon suggests new opportunities for modifying polyamide properties through post-polymerization alkene functionalization.

2.1.1 Mechanical characterization of the unfunctionalized PA66 MULCH copolymer. The thermal properties are detailed in Table 2. Across these thermal analyses, a notable consistency in thermal stability is observed, even with higher MULCH incorporations. T_m remained virtually unchanged and T_g decreased slightly between pure PA66 and its MULCH-modified counterparts. PA66-MULCH-10 exhibited an increased ΔH_m, indicating similar crystallization kinetics and enhanced crystallinity.

Tensile testing (Table 1) was performed after conditioning at 63% RH and 70 °C for 48 hours. The results align with established trends in the literature and validate our initial hypothesis, which contended that the addition of the MULCH model molecule would allow the conventional PA materials to

Table 2 Thermal data for unmodified polyamides

polyamide	T_m, °C	T_c, °C	ΔH_c, J g^{-1}	ΔH_m, J g^{-1}	T_g, °C
Neat polyamides					
PA66	261	222	54.6	59.3	64
PA66-MULCH-5	260	219	51.6	87.7	58
PA66-MULCH-10	257	209	50.6	87.9	53
Untreated fibers					
PA66	261	222	47.8	59.3	—
PA6	222	182	64.5	30.8	—
PA66-Blend-10	262	227	60.3	64.3	—
PA6-MULCH-10	203	164	50.9	58.5	—

retain their robust mechanical properties while still incorporating a new functional handle for further chemistry. Consistent with findings on long-chain polyamides like industrial PA 6,14,[47–49] an increase in chain length typically enhances the polymer's elasticity. Remarkably, PA66-MULCH-5 improved both ultimate tensile strength (UTS) as compared to PA66, along with a slight elongation enhancement, in spite of a reduced molecular weight. This minimal MULCH addition did not drastically alter mechanical properties compared to higher MULCH percentages. Such small MULCH additions potentially facilitate internal plasticization, contributing to greater strain hardening, increased chain mobility, and overall enhanced mechanical performance. This conclusion was further confirmed using statistical analysis. The *p*-values (Fig. S14a†) for the neat dogbone elongation at yield and break are both above 0.05, which indicates the addition of the MULCH did not significantly change the overall properties. While the UTS was statistically different, this can be attributed to the internal plasticization effect previously discussed.

2.2 Alkene functionalization using thiol-click reactions in solid-state copolyamides and blend polymers

After verifying the bio-enhanced polyamide's thermomechanical performance, investigating the alkene's reactivity and accessibility became the first task. Although the alkene endured the rigorous polymerization environment, its availability for subsequent chemical reactions in either solution or solid state remained uncertain. The limited solubility of polyamides, restricted to strong acids and select organic solvents such as *n*-cresol, curtails the scope of feasible solution state chemical reactions, diminishing their potential as versatile platform polymers. Moreover, scaling up solution state reactions is complicated by prolonged dissolution times and the need for large quantities of industrially dangerous chemicals. Conversely, the ability to chemically modify the alkene in the solid state would significantly expand the polymer's applicational horizon, removing necessary solvents and decreasing reaction times. Melt state reactions, performed in a twin-screw extruder or during polymerization, present another promising avenue for alkene functionalization, offering a potentially straightforward method for chemical modifications. However, this paper does not delve into melt-state reactions, focusing

instead on the solid-state possibilities and their implications for broadening the polyamide's utility.

To illustrate the reactivity of the alkene with respect to solid-state chemical processing, four additional polyamide samples were prepared at a sufficient scale to produce usable quantities of fiber. The properties of the materials after synthesis and melt spinning are outlined in Table 1. Samples are encoded with PA66 or PA6 prefixes to indicate the respective polyamide system. PA66/PA6-MULCH-*X* refers to PA66 or PA6 copolymerized with *X* wt% C20:1/HMDA salt. PA66-Blend is a physical blend of PA66-MULCH-40 and PA66 in a 5 : 1 mass ratio.

To assess the alkene's reactivity, two experimental approaches were employed. Initially, osmium tetroxide staining was employed as a qualitative measure of alkene accessibility due to its specificity for double bonds, providing a visual confirmation of alkene activity. Both PA66 and PA66-Blend fibers turned from white to brown upon staining, with the alkene-containing samples showing a notably darker hue, indicative of true reactivity, as documented in Fig. 3. To confirm the staining resulted from chemical interaction with the alkenes rather than mere physical deposition, the polymers were subjected to dissolution, precipitation, and drying. The alkene-modified polyamide remained stained, whereas the pure polyamide samples returned to their original white colour after washing, highlighting both the reactivity and accessibility of the alkene in the solid state.

This visual demonstration qualitatively showed the MULCH alkene was addressable in the solid state, at least with aggressive reactions using OsO_4. Finding milder, more practical chemistries capable of modifying the mechanical properties thus became the primary motivation. Epoxidation, a simple reaction foundational for many subsequent reactions,[50–54] was conducted on injection-molded dogbone PA66-MULCH-10. The ^{1}H NMR analysis of a dogbone section was performed on a 2 cm × 2 cm cross-section of the head of the dogbone. The head of the dogbone was cut cross-sectionally and then dissolved; ^{1}H NMR was used to analyze the amount of alkene consumed, as shown in Figure 2. This NMR revealed 65% alkene consumption, demonstrating excellent reactivity, well into the interior of the specimen. The consumption of most of the alkene, despite mass transfer limitations present in the solid state, shows the high reactivity and accessibility irrespective of thickness. Although direct evidence of epoxy ring formation was obscured by spectral overlap, the significant reduction in alkene peaks *via* ^{1}H NMR analysis from the epoxidation reaction underscored the potential for further exploratory experiments.

Having established the chemical reactivity of the alkene with respect to solid-state reactions, we turned our focus to chemical modifications hypothesized to result in property differentiation. The functionalization of the MULCH alkene was thus explored through the well-known thiol–ene "click" reaction. Two thiol-based compounds were selected, each targeting a specific property: one to boost hydrophobicity and the other to enhance mechanical strength *via* crosslinking. Dodecanethiol, with its twelve-carbon aliphatic chain, was selected to enhance hydrophobicity, and pentaerythritol tetrakis(3-mercaptopropionate) ("tetrakis") was used for crosslinking reactions, with the results shown in Fig. 4.

The objective was to evaluate the hydrophobicity impact of thiol additives on polyamide fibers, where traditional surface-area dependent contact angle measurement was impractical. Instead, hydrophobicity was assessed by weight gain, equating any increase in weight to water absorption, as shown in Table 1. Both virgin PA66-Blend and PA6-MULCH-10 demonstrated a significant decrease in water uptake as compared to PA66 and PA6. The subsequent addition of the dodecanethiol tail resulted in a further decrease in water uptake, demonstrating the ability to modify the hydrophobicity of the polymer. Additionally, this result demonstrates an intrinsic benefit to the MULCH monomer, as hydrophobicity is a built-in advantage without the need for further functionalization, freeing the alkene chemical handle to perform new property modifications, such as the ability to cross-link after processing and increase the mechanical strength significantly.

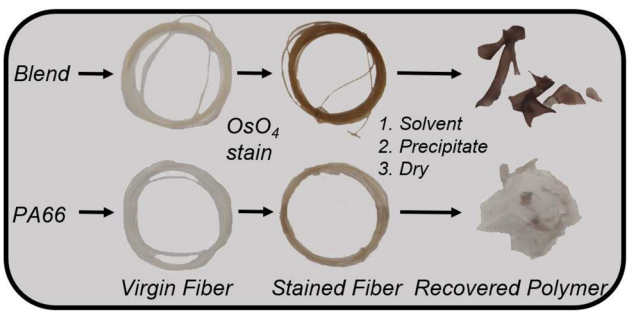

Fig. 3 Results of the OsO_4 staining technique. PA66-Blend fiber was stained alongside a pure PA66 fiber. Each fiber was exposed to OsO_4. To wash, they were dissolved in formic acid and reprecipitated in methanol. The fibers on the top correspond to the PA66-Blend stain, while the fibers on the bottom correspond to PA66. The final image in each line shows the results of the wash.

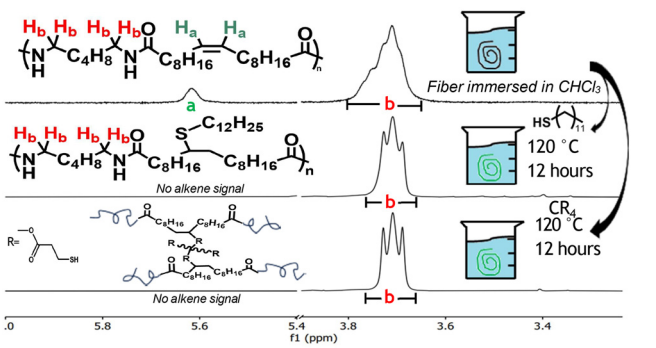

Fig. 4 NMR demonstrating complete alkene consumption in thiol–ene click reactions. The top figure shows the unmodified PA66-Blend, clearly displaying the alkene signal at 5.5 ppm. The second spectrum shows the alkene consumption with dodecanethiol, with the last spectra showing total alkene consumption with tetrakis.

Thus, further study of the property modification focused on the use of the tetrakis in cross-linking reactions. Once the thiol–ene reaction finished, the mechanical properties of the four unique fibers were evaluated to assess the impact of tetrakis thiol treatments, specifically looking for increases in UTS as an indicator of cross-linking due to enhanced resistance to plastic deformation. Any observed changes in the dodecanethiol-treated materials would provide further evidence the addition of a pendant group on the alkene site can alter mechanical properties. This assessment was performed on bundles of five fibers, with stress recalculated and adjusted for each fiber breakage, with results tabulated in Table 1. Notably, the industrial samples PA6-C12, PA6-SH_4, PA66-C12, and PA66-SH_4 showed no mechanical changes post-treatment, conclusively demonstrating the need for MULCH to differentiate properties. Dodecanethiol treatment notably improved UTS in the PA66-Blend sample. The comparison between the fibers treated with the tetrakis or dodecanethiol revealed a subtle impact from tetrakis treatment relative to dodecanethiol, which enhanced UTS, albeit at the cost of reduced elongation. This improvement is attributed to dodecanethiol's plasticization effect, where its long aliphatic chain facilitates quicker chain alignment, predisposing the material to strain-induced crystallization. PA6-MULCH-10 underwent significant oxidation during fiber extrusion, leading to a marked color change in the fibers and exhibited poor mechanical performance, showing the oxidation was enough to reduce the mechanical properties. The tetrakis treatment nonetheless provided conclusive evidence the addition of a thiol molecule was capable of modifying material properties in exciting ways. This conclusion is corroborated by statistical analysis. The *p*-values seen in Fig. S14b† shows there is a statistical significance between the various samples, demonstrating the addition of the small molecules does significantly change mechanical properties.

The series of alkene functionalization reactions yielded two key findings. First, they confirmed the alkene's accessibility. Three distinct chemistries—OsO_4 staining, epoxidation, and thiol–ene click—were applied to solid-state samples. Each method significantly reduced alkene concentration in the backbone, indicating the alkene's susceptibility to a broad spectrum of chemistries beyond those tested. Second, the thiol–ene reactions highlighted the alkene's potential for property differentiation. Adding new pendant groups positively and noticeably altered the mechanical properties, demonstrating the feasibility of modifying tensile properties through the careful selection of pendant groups and chemistries.

These two key findings highlight an enticing reality: alkene reactivity enables the development of a platform polyamide capable of addressing pertinent challenges in polyamide applications. By harnessing this bio-based alkene, a range of innovations becomes possible, including plasticizer tethering, bio-content incorporation for mechanical enhancements, chemical upcycling, and improved film design through tie-layer elimination. One immediate advantage is the ability to reduce plasticizer leaching, a pressing environmental concern. Sulfonamides are widely used in polyamide manufacturing for easier processing; however, they pose toxicity risks, particularly in marine environments.[55–58] By chemically anchoring sulfonamides to the polyamide backbone *via* alkene functionality, leaching can be minimized while preserving essential processing properties. Beyond plasticizer retention, alkene functionality offers pathways for modifying material properties, as discussed previously. The use of vegetable oils as pendant groups could enhance hydrophobicity and cross-linking density through long-chain thiol–ene click reactions. These modifications would expand polyamide applications across industries, from automotive to commercial fishing, without increasing reliance on petrochemicals. The same alkene group also enables chemical upcycling, addressing end-of-life concerns. Ozonolysis, for instance, could break down the long-chain diacid into a shorter diacid, allowing for repolymerization into a new product. The reduction in chain length would make it more comparable to PA66, broadening its suitability for PA66-like applications. This approach effectively doubles the material's lifespan—a particularly meaningful advancement considering polyamide-based plastics in transportation have an average lifespan of 13 years.[59] Extending this duration would significantly reduce landfill waste. Lastly, the polyamide's adaptability offers a solution to the recycling challenges posed by multilayer films. Current packaging designs rely on tie-layers to bond incompatible materials, making separation difficult and leading to widespread disposal in landfills.[60] The platform polyamide's alkene functionality enables direct chemical bonding between layers, eliminating the need for tie-layers and simplifying recycling. By integrating these advantages, this polyamide platform demonstrates a unique versatility—addressing environmental concerns, enhancing performance, and extending material longevity. Its potential reaches far beyond the scope of this work, laying the groundwork for future innovations.

3 Conclusion

This study investigated incorporating a model long-chain diacid unsaturated molecule, analogous to bio-derived molecules, into the backbone using copolymerization techniques to leverage the unique chemical moiety contained therein. We discovered the alkene, positioned within the diacid, withstands the rigorous polymerization process, enabling post-polymerization modifications. Thermomechanical evaluations revealed the modified polyamide's properties are on par with or exceed those of conventional industrial polyamides, with thermal properties showing a negligible difference in melting temperatures of less than 5 °C and mechanical analysis indicating enhanced toughness. Further investigations confirmed the alkene's solid-state accessibility, employing various chemical strategies for functional group integration aimed at property enhancement. Initial experiments with osmium tetroxide visually confirmed alkene accessibility, while epoxidation reactions, validated through NMR, underscored the feasibility of

chemical accessibility. Efforts to enhance mechanical properties using thiol-click chemistry with both multi-thiol and mono-thiol chemicals showed increases in UTS with decreases in elongation. These experiments effectively showcased the alkene's accessibility and the polymer's modifiability, establishing it as a versatile polymer platform. Future directions include identifying optimal chemicals for targeted property modifications. The MULCH monomer emerges as a bio-based component, which transforms polyamides into a platform with vast potential to overcome prevalent challenges, such as water absorption and mechanical degradation. This innovative polyamide platform's future applications are limited only by engineering creativity and the specific challenges at hand. With strategic development and application, this novel polyamide could offer comprehensive solutions to the industry's pressing issues.

4 Experimental section

4.1 Materials

10-Undecenoic acid, adipic acid, dodecanethiol, osmium tetroxide, dicumyl peroxide, trifluoroacetic anhydride (TFAA), *meta*-chloroperbenzoic acid (mCPBA), and pentaerythritol tetrakis (3-mercaptopropionate), abbreviated as tetrakis, were purchased from Sigma-Aldrich and used as received. The second-generation Grubbs was purchased from Abaci Pharma and used as received.

4.2 Synthesis and characterization

4.2.1 NMR collection and analysis. Small molecule conversion and purity were monitored using ^{1}H NMR spectra. The spectra were collected with either a Bruker Neo 400 or a Varian MR-400 and analyzed with MestReNova software using either D_2O or CDCl3 as a solvent. Polyamide samples were dissolved in a 2 : 1 (v/v) ratio of CDCl3 and TFAA. ^{13}C NMR was run on a Bruker Neo 400 with the same preparation but additionally adding 100 μL of chromium(III) acetylacetonate to the solution.

4.2.2 Molecular weight analysis. Polyamide molecular weight was characterized using gel permeation chromatography with a Tosoh Ecosec HLC-8320GPC equipped with UV and RI detectors and using hexafluoroisopropanol (HFIP) as the eluent. The concentration of samples was 10 mg mL^{-1} in HFIP and poly(methyl methacrylate) (PMMA) standards were used.

4.2.3 Differential scanning calorimetry. The thermal properties were analyzed with a Thermal Analysis Discovery 2500 DSC in a nitrogen environment. The samples were first annealed by ramping the temperature from 40 °C to 120 °C at a rate of 20 °C min^{-1} and holding it at 120 °C for 2 hours to remove any previous thermal history. Three heat cycles from 25 °C to 300 °C at a rate of 10 °C min^{-1} were performed. The results from the third cycle were reported. Modulated DSC (mDSC) was run with an amplitude of 1.27 °C at a rate of 2 °C min^{-1} with an isothermal step of 5 minutes. The glass transition temperature was determined using a TA Ares G2 rheometer with a tension fixture, oscillating at 10 rad s^{-1} from 0 °C to 100 °C.

4.2.4 Thermogravimetric analysis. TGA was run on a Netzsch STA 449 F1 Jupiter system with alumina pans. The system ramped from 40 °C to 1000 °C at a rate of 10 °C min^{-1} under a flow of nitrogen.

4.2.5 Second generation Grubbs-facilitated metathesis of 10-undecenoic acid. The long chain diacid was synthesized *via* a self-metathesis reaction under inert conditions using a 0.05 wt% second-generation Grubbs catalyst. The catalyst was added to 10-undecenoic acid in an inert environment. The solution was heated to 50 °C for 24 hours in a 1.3 L Col-Int Tech stirred high-pressure reactor with a constant argon sweep. The product was removed and washed three times with hexane at 0 °C and five times with boiling hexane, with purity checked between washes with ^{1}H NMR. The washes ceased when the product reached monomer purity levels.

4.2.6 Salt formation, polymerization, and melt processing of polyamides. The PA66 salt was prepared in a 5 gallon bucket equipped with a water chilling coil and an IKA RW 20 digital overhead agitator. 1.8 kg of adipic acid was dissolved in 4 L of methanol. 1.02 molar equivalents (1.5 kg) of HMDA were dissolved into 4 L of methanol. The two mixtures were slowly combined to maintain a constant 50 °C temperature. The mixture was mixed for 16 hours, agitating at 500 RPM. The salt was then filtered and washed with warm methanol to remove excess adipic acid and HMDA. Purity was checked *via* ^{1}H NMR analysis. The process to prepare the PA6,20:1 salt was similar, although conducted on a smaller scale. 41 g of the long-chain diacid (10-icosenedioic acid) was added to a 1 L round bottom flask equipped with an IKA RW 20 digital overhead stirrer. The reaction flask was placed into a cooling bath and 500 mL of ethanol was added. 1.05 stoichiometric equivalents of the HMDA were dissolved in 423 mL of ethanol. The bath was heated to 45 °C and ran for 1 hour. The solution was filtered with a Büchner funnel and washed with hot ethanol four times.

The polyamidation was performed in a 100 mL Col-Int high pressure stirring reactor, which is temperature controlled with an external thermocouple.[45] This is a delicate operation; please see ref. 41 for more details. However, in brief, 28 g of PA66 salt or ε-caprolactam was combined with 10 wt% (2.8 g) of the MULCH salt and 60 wt% (18.48 mL) water. The vessel was inerted and pressurized (P_0 = 70 psi) with argon. The temperature was set to 325 °C for 3 hours under agitation, the steam was removed, and the temperature was set to 400 °C for 2 hours. The unfunctionalized dog bones were injection molded using a HAAKE MiniJet Pro injection molder with a barrel temperature of 270 °C. The MULCH substituted polyamides were formed into four different fibers and prepared using a Thermo Scientific Process 11 parallel twin-screw extruder. Industrial PA6 and PA66 as well as the PA6-MULCH-10 were extruded at 275 °C in an inert argon environment using a 1 mm die. A blend material was extruded using industrial PA66 and laboratory made PA66-*co*-620:1. Using conditions similar to those of the PA66 fiber extrusion, 28 g PA66 and

5.6 g PA66-*co*-620:1 were combined in batches to produce a homogeneous fiber.

4.2.7 Water uptake. Five 2 inch fibers of each sample were dried for 24 hours in a vacuum oven at 70 °C. They were weighed collectively and placed in a fully aqueous environment under ambient conditions for 48 hours. They were then removed, dried down with a towel, and weighed again. The percent difference between the initial and final weight was calculated.

4.2.8 Tensile testing. The mechanical properties were tested on a Universal Testing Machine from Guangdong Liyi Technology Co with a strain rate of 10 mm min^{-1}. Fibers were tested in aggregate with five fibers per test. The experiment continued until all 5 fibers broke. The strain was calculated from the force given and divided by the number of fibers. The strain was manually adjusted each time a fiber broke to account for the loss in cross-sectional area to create a constant curve.

4.3 Post-polymerization modification

4.3.1 Osmium tetroxide staining. A coil was made from all four sample types: industrial PA6 and PA66, PA6-MULCH-10, signifying the 10 wt% MULCH addition, and PA66-Blend, signifying the blended nature of a concentrated MULCH copolymer with industrial PA66. The strands were suspended above tetroxide for 4 hours. The chemical binding of the osmium tetroxide was tested by dissolving the coils in formic acid, followed by recovery, filtration, and drying.

4.3.2 Epoxidation. The epoxidation reaction was performed on previously mechanically tested dogbones. The grip section of the dogbone was snipped off. A solution of 5 g of mCPBA and 10 g of water was prepared and heated to 50 °C. The dogbone piece was immersed in the solution for 10 hours. It was removed, dried, and cut cross-sectionally and then analyzed using ^{1}H NMR techniques.

4.3.3 Thiol-click chemistry. Post-polymerization modifications were analysed for all four samples. Ten 2 inch fibers of each sample were cut and soaked in a mixture of 40 mL of chloroform and 2 g of dicumyl peroxide for 24 hours at room temperature. Five fibers were then used to perform thiol click reactions using two different thiol based molecules: dodecanethiol and pentaerythritol tetrakis (3-mercaptopropionate). 40 mL of each were prepared and 5 prepared fibers were placed into the bath and then purged for 10 minutes with argon. The bath was then heated to 120 °C for 16 hours with a magnetic stirrer at 100 rpm. After the reaction, the fibers were placed into a clean chloroform bath for 24 hours and then dried using a vacuum oven.

4.3.4 Statistical analysis of tensile data. The UTS and elongation data were extracted, and then means and standard deviations were calculated to provide descriptive statistics. The statistical significance of differences between samples was evaluated using a one-way analysis of variance (ANOVA). The null hypothesis is all sample means are equal. The *p*-value corresponds to the probability of observing an *F*-statistic at least as extreme as the one calculated. Here, a threshold of $\alpha = 0.05$ was used to determine the significance. If $p < 0.05$, then at least one sample's mean differs from the others at the 95% confidence level. Detailed results, including *F*-statistics and *p*-values for each measured property (UTS, strain at UTS, and final strain), are summarized in Fig. S14.† All analyses were performed with Python or equivalent statistical software.

Author contributions

Peter M. Meyer: methodology, formal analysis, investigation, writing – original draft, writing – review & editing, and visualization. Dhananjay Dileep: resources, data curation, and methodology. Risha L. Bond: conceptualization, methodology, formal analysis, resources, project administration, and software. Fasil A. Tadesse: formal analysis, resources, project administration, and software. Michael J. Forrester: conceptualization, methodology, software, formal analysis, investigation, data curation, and writing – review & editing. Eric W. Cochran: writing – original draft, writing – review & editing, visualization, conceptualization, methodology, validation, formal analysis, resources, data curation, software, project administration, funding acquisition, and securing funding.

Data availability

Data for this article, including raw data and images, are available at Harvard Dataverse at **https://doi.org/10.7910/DVN/OEULEA**.

Conflicts of interest

There are no conflicts to declare.

Acknowledgements

This work was supported and funded by REG Life Sciences, the NSF Center for Bioplastics and Biocomposites (CB^2 NSF Award #2113695) and by Genomatica.

References

1 H. L. Fisher, *J. Chem. Educ.*, 1941, **18**, 99.
2 Polyamides – Still Strong After Seventy Years – Marchildon – 2011 – Macromolecular Reaction Engineering – Wiley Online Library, **https://onlinelibrary.wiley.com/doi/10.1002/mren.201000017**.
3 Biobased Polyamides: Recent Advances in Basic and Applied Research – Winnacker – 2016 – Macromolecular Rapid Communications – Wiley Online Library, **https://onlinelibrary.wiley.com/doi/10.1002/marc.201600181**.
4 M. Vojdani and R. Giti, *J. Dent.*, 2015, **16**, 1–9.

5 M. Shakiba, E. Rezvani Ghomi, F. Khosravi, S. Jouybar, A. Bigham, M. Zare, M. Abdouss, R. Moaref and S. Ramakrishna, *Polym. Adv. Technol.*, 2021, **32**, 3368–3383.
6 P. H. Nguyen, S. Spoljaric and J. Seppälä, *Eur. Polym. J.*, 2018, **109**, 16–25.
7 F. Stempfle, P. Ortmann and S. Mecking, *Chem. Rev.*, 2016, **116**, 4597–4641.
8 K. S. Louise and M. P. Winthrop, Process for the production of a highly orientable, crystallizable, filament-forming polyamide, *US Patent and Trademark Office*, US3287323A, 1966, **https://patents.google.com/patent/US3287323A/en**.
9 R. R. Pal, P. S. Patil, M. M. Salunkhe, N. N. Maldar and P. P. Wadgaonkar, *Eur. Polym. J.*, 2009, **45**, 953–959.
10 P. Estévez, H. El-Kaoutit, F. C. García, F. Serna, J. L. de la Peña and J. M. García, *J. Polym. Sci., Part A: Polym. Chem.*, 2010, **48**, 3823–3833.
11 N. San-José, A. Gómez-Valdemoro, F. C. García, F. Serna and J. M. García, *J. Polym. Sci., Part A: Polym. Chem.*, 2007, **45**, 4026–4036.
12 Soluble Polyamides and Polyimides Functionalized with Benzo-5-Crown-5-Pendant Groups – Maya – 2004 – Macromolecular Rapid Communications – Wiley Online Library, **https://onlinelibrary.wiley.com/doi/10.1002/marc.200300092**.
13 K. Su, N. Sun, X. Tian, X. Li, D. Chao, D. Wang, H. Zhou and C. Chen, *Mater. Today Chem.*, 2021, **22**, 100536.
14 M. Winnacker, *Biomater. Sci.*, 2017, **5**, 1230–1235.
15 Thermally Reversible Cross-Linked Polyamides with High Toughness and Self-Repairing Ability from Maleimide- and Furan-Functionalized Aromatic Polyamides – Liu – 2007 – Macromolecular Chemistry and Physics – Wiley Online Library, **https://onlinelibrary.wiley.com/doi/10.1002/macp.200600445**.
16 Y. Zhu, C. Romain and C. K. Williams, *Nature*, 2016, **540**, 354–362.
17 Z. Wang, M. S. Ganewatta and C. Tang, *Prog. Polym. Sci.*, 2020, **101**, 101197.
18 Modern biopolyamide-based materials: synthesis and modification | Polymer Bulletin, **https://link.springer.com/article/10.1007/s00289-019-02718-x**.
19 M. Alam, D. Akram, E. Sharmin, F. Zafar and S. Ahmad, *Arabian J. Chem.*, 2014, **7**, 469–479.
20 Vegetable oil-based thermosetting polymers – Galia – 2010 – European Journal of Lipid Science and Technology – Wiley Online Library, **https://onlinelibrary.wiley.com/doi/10.1002/ejlt.200900096**.
21 R. Ahorsu, F. Medina and M. Constantí, *Energies*, 2018, **11**, 3366.
22 T. Yu, Y. J. Zhou, L. Wenning, Q. Liu, A. Krivoruchko, V. Siewers, J. Nielsen and F. David, *Nat. Commun.*, 2017, **8**, 15587.
23 N. Kolb, M. Winkler, C. Syldatk and M. A. R. Meier, *Eur. Polym. J.*, 2014, **51**, 159–166.
24 R. Akbari Javar, M. I. Bin Noordin, M. Khoobi and A. Ghaedi, *J. Inorg. Organomet. Polym. Mater.*, 2020, **30**, 2520–2532.
25 M. A. R. Meier, J. O. Metzger and U. S. Schubert, *Chem. Soc. Rev.*, 2007, **36**, 1788–1802.
26 L. Maisonneuve, T. Lebarbé, E. Grau and H. Cramail, *Polym. Chem.*, 2013, **4**, 5472–5517.
27 Biotechnological synthesis of long-chain dicarboxylic acids as building blocks for polymers – Huf – 2011 – European Journal of Lipid Science and Technology – Wiley Online Library, **https://onlinelibrary.wiley.com/doi/10.1002/ejlt.201000112**.
28 Synthesis and Characterization of New Soluble Cardo Aromatic Polyamides Bearing Diphenylmethylene Linkage and Norbornyl Group – Liaw – 2001 – Macromolecular Chemistry and Physics – Wiley Online Library.
29 C. Schilling, *Ind. Biotechnol.*, 2022, **18**, 63–65.
30 R. P. Elander, *Appl. Microbiol. Biotechnol.*, 2003, **61**, 385–392.
31 D. R. Vardon, N. A. Rorrer, D. Salvachúa, A. E. Settle, C. W. Johnson, M. J. Menart, N. S. Cleveland, P. N. Ciesielski, K. X. Steirer, J. R. Dorgan and G. T. Beckham, *Green Chem.*, 2016, **18**, 3397–3413.
32 Chemical Routes for the Transformation of Biomass into Chemicals | Chemical Reviews, **https://pubs.acs.org/doi/10.1021/cr050989d**.
33 W. Niu, K. Draths and J. Frost, *Biotechnol. Prog.*, 2002, **18**, 201–211.
34 N. Hernández, R. C. Williams and E. W. Cochran, *Org. Biomol. Chem.*, 2014, **12**, 2834–2849.
35 M. Suastegui, J. E. Matthiesen, J. M. Carraher, N. Hernandez, N. Rodriguez-Quiroz, A. Okerlund, E. W. Cochran, Z. Shao and J.-P. Tessonnier, *Angew. Chem., Int. Ed.*, 2016, **55**, 2368–2373.
36 J. M. Carraher, P. Carter, R. G. Rao, M. J. Forrester, T. Pfennig, B. H. Shanks, E. W. Cochran and J.-P. Tessonnier, *Green Chem.*, 2020, **22**, 6444–6454.
37 J. Hadel, S. Noreen, M. N. Dell'anna, D. Dileep, B. H. Shanks, J.-P. Tessonnier and E. W. Cochran, ACS Symposium Series, American Chemical Society, Washington, DC, 2023, vol. 1451, pp. 163–176.
38 J. B. J. H. van Duuren, B. Brehmer, A. E. Mars, G. Eggink, V. A. P. M. Dos Santos and J. P. M. Sanders, *Biotechnol. Bioeng.*, 2011, **108**, 1298–1306.
39 S. C. Mokwatlo, B. C. Klein, P. T. Benavides, E. C. D. Tan, C. M. Kneucker, C. Ling, C. A. Singer, R. Lyons, V. Sànchez i Nogué, K. V. Hestmark, M. A. Ingraham, K. J. Ramirez, C. W. Johnson, G. T. Beckham and D. Salvachúa, Bioprocess development and scale-up for cis,cis-muconic acid production from glucose and xylose by Pseudomonas putida, *Green Chem.*, 2024, **26**, 10152–10167.
40 R. S. Nelson, E. P. Knoshaug, R. Spiller, N. Nagle, S. VanWychen, M. Wiatrowski, R. Davis, P. T. Pienkos and J. S. Kruger, *Algal Res.*, 2023, **75**, 103300.
41 A. Corona, M. J. Biddy, D. R. Vardon, M. Birkved, M. Z. Hauschild and G. T. Beckham, Life cycle assessment of adipic acid production from lignin, *Green Chem.*, 2018, **20**, 3857–3866.

42 P. Carter, J. L. Trettin, T.-H. Lee, N. L. Chalgren, M. J. Forrester, B. H. Shanks, J.-P. Tessonnier and E. W. Cochran, *J. Am. Chem. Soc.*, 2022, **144**, 9548–9553.
43 M. Scholl, T. M. Trnka, J. P. Morgan and R. H. Grubbs, *Tetrahedron Lett.*, 1999, **40**, 2247–2250.
44 T. S. Jahnke, *J. Am. Chem. Soc.*, 1996, **118**, 8186–8186.
45 P. M. Meyer, M. Forrester and E. W. Cochran, *Ind. Eng. Chem. Res.*, 2024, **63**, 19506–19514.
46 S. Abdolmohammadi, D. Gansebom, S. Goyal, T.-H. Lee, B. Kuehl, M. J. Forrester, F.-Y. Lin, N. Hernández, B. H. Shanks, J.-P. Tessonnier and E. W. Cochran, *Macromolecules*, 2021, **54**, 7910–7924.
47 R. Sattler, V. Danke and M. Beiner, *Macromol. Chem. Phys.*, 2023, **224**, 2200433.
48 J. Jiang, Q. Tang, X. Pan, Z. Xi, L. Zhao and W. Yuan, *Ind. Eng. Chem. Res.*, 2020, **59**, 17502–17512.
49 M. Ehrenstein, S. Dellsperger, C. Kocher, N. Stutzmann, C. Weder and P. Smith, *Polymer*, 2000, **41**, 3531–3539.
50 A. H. N. Armylisas, M. F. S. Hazirah, S. K. Yeong and A. H. Hazimah, *Grasas Aceites*, 2017, **68**, e174.
51 E. Blée and F. Schuber, *J. Biol. Chem.*, 1990, **265**, 12887–12894.
52 G. Grigoropoulou, J. H. Clark and J. A. Elings, *Green Chem.*, 2003, **5**, 1–7.
53 H. Yao and D. E. Richardson, *J. Am. Chem. Soc.*, 2000, **122**, 3220–3221.
54 J. Salimon, N. Salih and E. Yousif, *J. Saudi Chem. Soc.*, 2011, **15**, 195–201.
55 W. Baran, J. Sochacka and W. Wardas, *Chemosphere*, 2006, **65**, 1295–1299.
56 H. S. J. Bergen and J. K. Craver, *Ind. Eng. Chem.*, 1947, **39**, 1082–1087.
57 A. Ovung and J. Bhattacharyya, *Biophys. Rev.*, 2021, **13**, 259–272.
58 R. Jamarani, H. C. Erythropel, J. A. Nicell, R. L. Leask and M. Marić, *Polymers*, 2018, **10**, 834.
59 R. Geyer, J. R. Jambeck and K. L. Law, *Sci. Adv.*, 2017, **3**, e1700782.
60 K. Kaiser, M. Schmid and M. Schlummer, *Recycling*, 2017, **3**, 1.